Supplementary Information

Confinement of poly(ethylene oxide) in the nanometer-scale pores of resins and carbon nanoparticles

Fabienne Barroso-Bujans,*[a,b] Pablo Palomino[c], Silvina Cerveny[a,b], Felix Fernandez-Alonso[d,e], Svemir Rudić[d], Angel Alegría[a,f], Juan Colmenero[a,b,f] and Eduardo Enciso[c]

Materials

The following compounds were used: resorcinol [($C_6H_4(OH)_2$), Sigma Aldrich, 99%], formaldehyde [(H_2CO), Panreac, 37-38% solution], sodium hydroxide [(NaOH), Sigma Aldrich, > 97%), deionized water (obtained from a Direct Q5 Millipore systems), and polyethylene oxide [(PEO), Aldrich, M_n=9.4x10^4 g/mol and polydispersity index 1.08].

Methods

R−Np was synthesized by polycondensation of resorcinol and formaldehyde following the approach of Pekala et al.[1] The reaction was performed in an aqueous solution containing 1.5 M resorcinol and 6 M formaldehyde. Sodium hydroxide was added to reach a pH of 6,7. Subsequently, the solution was placed in an oven at 85 ºC for three days. The colour of the solution changed progressively from clear to orange, then to red, and finally to dark brown over the course of the reaction. These colour changes presumably originate from an increasing degree of electronic π-delocalization of fused benzenoid rings in the material. Gelation was achieved in 80 min. After curing, the gel was dried at 85 ºC at ambient pressure over the course of two additional days, leading to a dry R−Np specimen. Finally, partially coalesced amorphous carbon nanoparticles (AC−Np) were obtained by pyrolysis of R−Np at 900 ºC for 4 hours in a N_2 atmosphere using a heating rate of 3 ºC/min and a cooling rate of 5 ºC/min.

[a]*Centro de Física de Materiales-Material Physics Center (CSIC-UPV/EHU), Paseo Manuel Lardizábal 5, 20018 San Sebastián, Spain. Fax: +34 94301 5800; Tel: +34 943018803, E-mail: fbarroso@ehu.es*
[b]*Donostia International Physics Center (DIPC), Paseo Manuel Lardizábal 4, 20018 San Sebastián, Spain.*
[c]*Departamento de Química Física I, Facultad de Ciencias Químicas, Universidad Complutense, 28040 Madrid, Spain. Fax +34 914944135; Tel: 34 913944211, E-mail enciso@quim.ucm.es*
[d]*ISIS Facility, Rutherford Appleton Laboratory, Chilton, Didcot, Oxfordshire, OX11 0QX, United Kingdom*
[e]*Department of Physics and Astronomy, University College London, Gower Street, London, WC1E 6BT, United Kingdom*
[f]*Departamento de Física de Materiales, Universidad del País Vasco (UPV/EHU), Apartado 1072, 20080 San Sebastián, Spain*

The chemical composition of resins and carbons was obtained by elemental analysis. The texture and porosity of dried, pyrolyzed, and PEO-filled carbons and resins were analysed by field-emission scanning electron microscopy (FESEM) and nitrogen adsorption-desorption isotherms.[2] FESEM images were collected with a JSM-6335F unit operating at 5 or 10 keV and 12 μA. Sample powders were supported on adhesive carbon tape and coated with a thin gold film. Nitrogen isotherms were obtained at 77 K using an ASAP 2020 from Micromeritics. AC−Np's were outgassed at 180 ºC for 1 hour, and R−Np's and PEO-containing samples were outgassed at 110 ºC for 6 hours. The specific surface area (S_{BET}) was determined form the linear part of the BET plot over the range P/P_0=0.05-0.25.[3] An example of this procedure is shown in Fig. S1. S_{BET} was obtained from the relation:

$$S_{BET} = n_m N_A \sigma$$

where n_m are the nitrogen moles required for coating the substrate in a monolayer, N_A is the Avogadro's number, and σ is the average area occupied by each nitrogen molecule (0.162 nm^2).[2] n_m is evaluated from the slope s and intercept i of the BET plot

$$n_m = \frac{1}{V_m(s+i)}$$

where V_m is the molar volume of nitrogen at STP conditions. External-surface (S_{ext}) and micropore (S_{mic}) areas were determined from the *t*-plots obtained via recourse to the Harkins and Jura equation:[4]

$$t = \left[\frac{13.99}{(0.034 - \log(\frac{P}{P_0}))} \right]^{1/2}$$

where t is the thickness of the adsorbed layer on the pore wall (see Fig. S2 for an example). The adsorbed amounts of nitrogen (V) *vs* thickness show a linear dependence in the t range 0.4-0.7 which allows us to estimate S_{ext} according to the equation:

$$S_{ext} = \frac{M}{\rho V_m}\frac{V}{t}$$

where M is the molar mass of nitrogen and ρ is the density of liquid nitrogen at 77 K (0.809 g/cm^3). S_{mic} is obtained by subtracting S_{ext} from S_{BET} Average pore diameters (d), mesopore volumes (V_{BJH}), and pore-size distributions (PSD's) were calculated with the Barrett-Joyner-Halenda (BJH) adsorption-desorption method[5] assuming cylindrical pores in the Kelvin equation.[6]

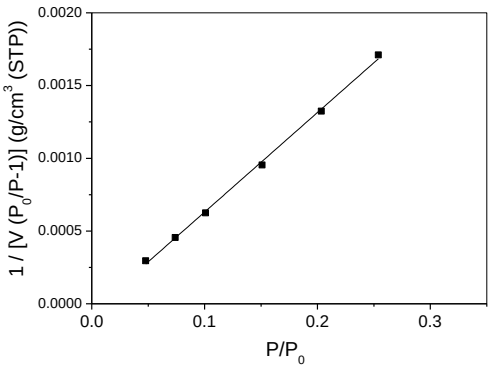

Fig. S1 BET plot of the nitrogen isotherm for AC-Np.

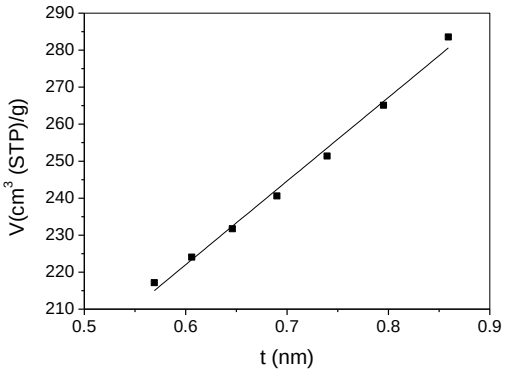

Fig. S2 t-plot of the nitrogen isotherm for AC-Np.

Thermogravimetric analysis (TGA) was carried out on a TA Instruments Q500 thermogravimetric analyzer. Samples were heated from room temperature to 800 ºC at a rate of 10 ºC/min under a constant N_2 flow of 60 mL/min. The amount of PEO in PEO/AC−Np and PEO/R−Np was calculated from sample-residue analysis at 800 ºC.

Inelastic neutron-scattering (INS) data were collected on the TOSCA spectrometer[7] located at the ISIS Facility, Rutherford Appleton Laboratory, U.K. TOSCA is a so-called indirect geometry time-of-flight neutron spectrometer spanning an energy-transfer range up to 8000 cm^{-1} in neutron energy loss with a spectral resolution of ~1.5%. INS time-of-flight spectra were collected in both back- and forward-scattering geometries, and then added together to obtain hydrogen-projected vibrational density of states (VDOS's). Typical run times varied between 2 and 8 h depending on the hydrogen content of the sample. All samples were contained in flat aluminum cells of thickness 1−4 mm and cooled to temperatures below 20 K. Emtpy-cell contributions to all raw INS spectra (both PEO-containing and pristine samples) were also subtracted prior to any further data analysis. The INS data for PEO shown in Fig.4a of the article were normalized to sample mass and those of PEO/GO and PEO/AC-Np were normalized to the amount of PEO content in the sample, as determined by TGA. The INS data in Fig. 4b of the main text were obtained by subtraction of the contribution from the AC-Np substrate shown in Fig. 4a.

Differential scanning calorimetry (DSC) measurements were carried out on ~12 mg specimens using a Q2000 TA Instruments in both standard and temperature-modulated (TM) modes. Standard DSC measurements were performed by placing the samples in sealed aluminum pans and cooling to 100 K at the highest attainable cooling rate, holding the temperature for 10 min at 100 K. Then, samples were heated back to 373 K at 30 K/min. This cooling-heating cycle was repeated two additional times with the same cooling rate and heating rates of 20 K/min and 10 K/min. To measure reverse heat flows following TM-DSC cooling runs, samples were heated back to 373 K at 5 K/min with a 0.48 K temperature amplitude and a 60-second modulation period. A helium-flow rate of 25 mL/min was used all throughout. TM-DSC data of bulk PEO was obtained from a pre-quenched sample. To this end, bulk PEO was melted on a hot plate at 353 K and then quenched in liquid nitrogen before introducing it into the measurement DSC cell.

Scanning Electron Microscopy

Comparison between SEM images of R-Np and AC-Np shows a highly compacted granular texture in both samples (Fig. S3). SEM images of PEO-filled samples show the absence of bulk PEO outside the grains (Fig. S4).

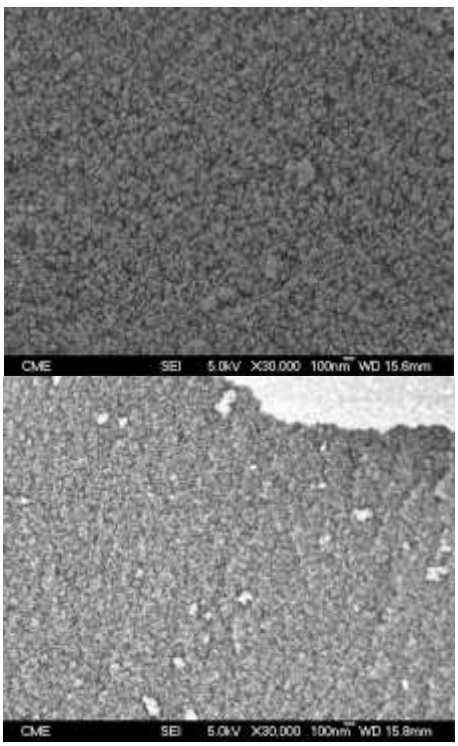

Fig. S3 SEM images of R-Np (top) and AC-Np (bottom).

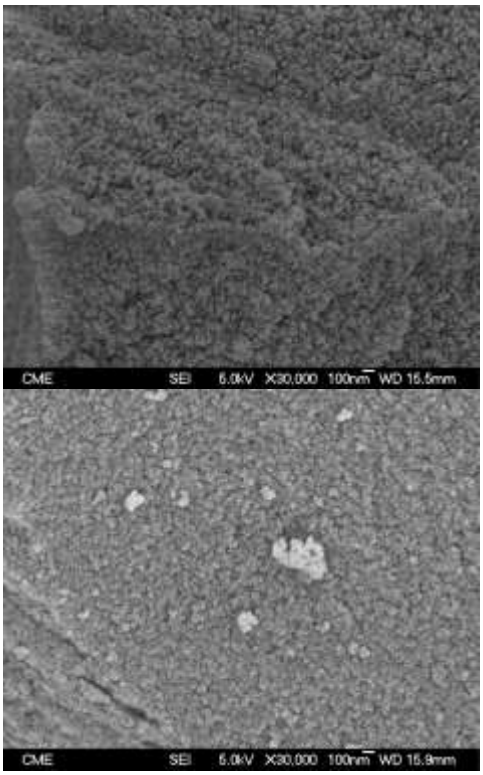

Fig. S4 SEM images of PEO/R-Np (top) and PEO/AC-Np (bottom).

Nitrogen Physisorption

Nitrogen adsorption-desorption isotherms for R-Np and PEO/R-Np are shown in Fig. S5 and those for AC-Np and PEO/AC-Np are shown in Fig. S6.

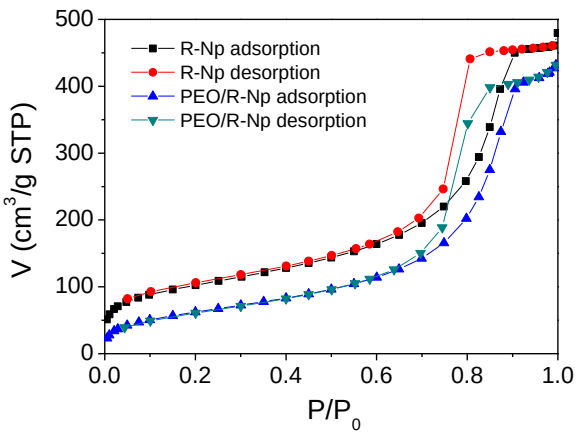

Fig. S5 Nitrogen adsorption-desorption isotherms for R−Np and PEO/R−Np.

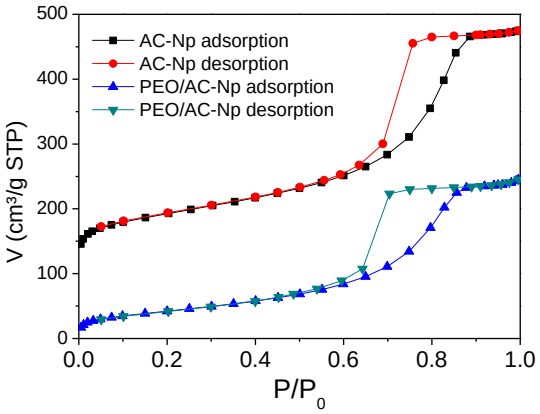

Fig. S6 Nitrogen adsorption-desorption isotherms for AC−Np and PEO/AC−Np.

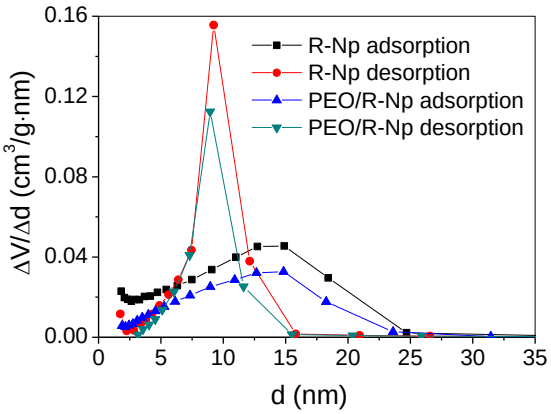

Fig. S7 PSD's for R−Np and PEO/R−Np.

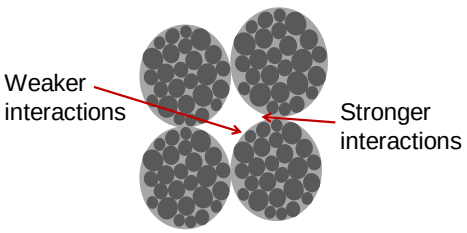

Fig. S8 Schematic drawing showing the small mesopores formed at inter-particle contacts. At these sites, polymer-substrate interactions are expected to be stronger than on free mesopore surfaces.

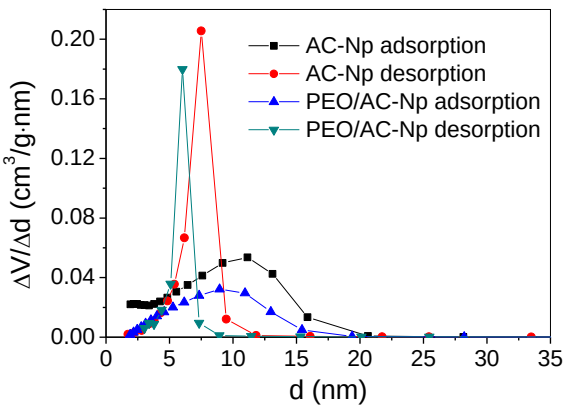

Fig. S9 PSD's for AC−Np and PEO/AC−Np.

Differential Scanning Calorimetry

DSC experiments in standard mode at relatively high heating rates (10-30 K/min) were also performed in order to increase our sensitivity to weak thermal events. DSC data for PEO/AC-Np (Fig. S10) show a change in the heat-flow signal at the Tg of bulk PEO. This heat-flow change is more pronounced as a function of heating rate, confirming the occurrence of a glass transition in the confined PEO. The onset and offset temperatures obtained from these data are reported in Table S1.

Table S1 Tg's of confined PEO in AC-Np and R-Np obtained from DSC at a series of heating rates.

	Heating rate (K/min)	Onset Tg ±5 (K)	Offset Tg ±5 (K)
Bulk PEO	3	212	224
	5	205	225
PEO/AC-Np	3	201	244
	5	201	249
	10	195	269
	20	195	253
	30	195	256
PEO/R-Np	10	194	-
	20	194	-
	30	192	249

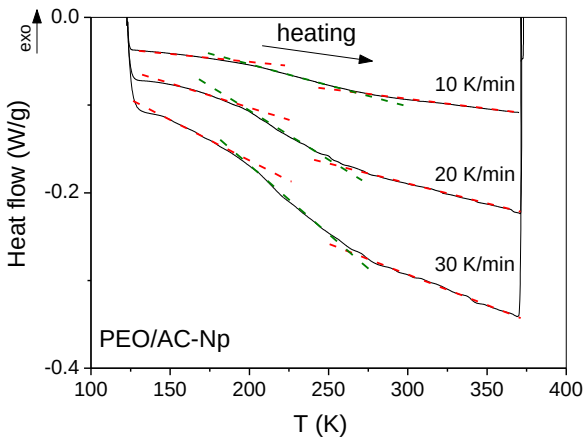

Fig. S10 Heating cycles of PEO/AC-Np during the DSC measurements.

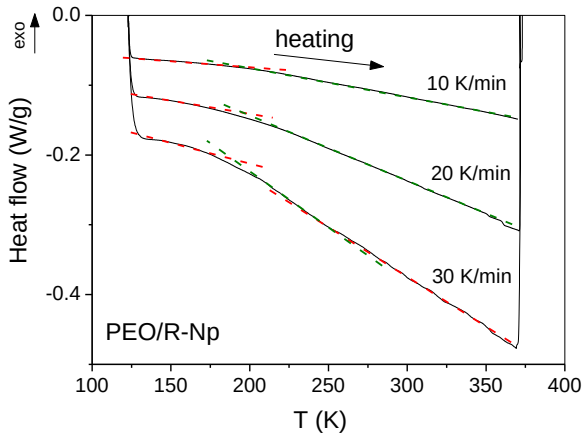

Fig. S11 Heating cycles of PEO/R-Np during the DSC measurements.

Similar experiments were conducted on PEO/R-Np (Fig. S11). In this case, changes in heat flow are hardly visible at low heating rates. A weak signal change appears at 20 K/min, becoming substantially more apparent at 30 K/min. The onset temperature of this process is similar to the one observed for PEO/AC-Np, as shown in Table S1. Offset temperatures could not be determined for this sample at 10 and 20 K/min.

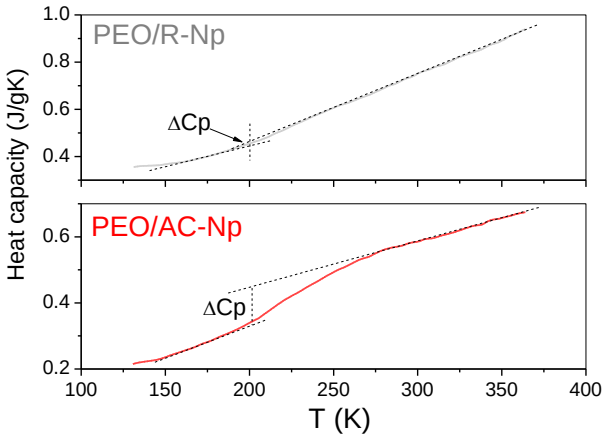

Fig. S12 Specific heat capacity of PEO/AC-Np and PEO/R-Np (both normalised to sample mass), obtained from a heating cycle at a rate of 30 K/min.

To account for possible contributions from the substrate to the DSC data, reversible heat-flow (*HF*) curves for PEO/AC-NP and PEO/R-Np ($HF_{PEO/Np}$) in the glass-transition region were calculated using the equation:

$$HF_{PEO/Np} = f_{PEO} HF_{PEO}^{amorphous} + f_{Np} HF_{Np}$$

where f_{PEO} and f_{Np} are the fractions of PEO and substrate nanoparticles (Np) in the sample, respectively, and HF_{Np} is the experimental *HF* of the Np. Owing to the tendency of bulk PEO to crystallize even upon quenching, experimental DSC data for entirely amorphous PEO ($HF^{amorphous}_{PEO}$) are not available. An approximation to this data was obtained by dividing the experimental *HF* of semicrystalline PEO ($HF^{semicrystalline}_{PEO}$) by the corresponding fraction of amorphous phase, which was determined to be only 40%. Including this approximation into the equation above, the *HF* can be written as:

$$HF_{PEO/Np} = \frac{f_{PEO} HF_{PEO}^{semicrystalline}}{0.4} + f_{Np} HF_{Np}$$

The results of this comparison are shown in Figs. S13a and b. For clarity, the data for the melting of PEO were removed from these *HF* traces, as they are of no relevance to the present discussion.

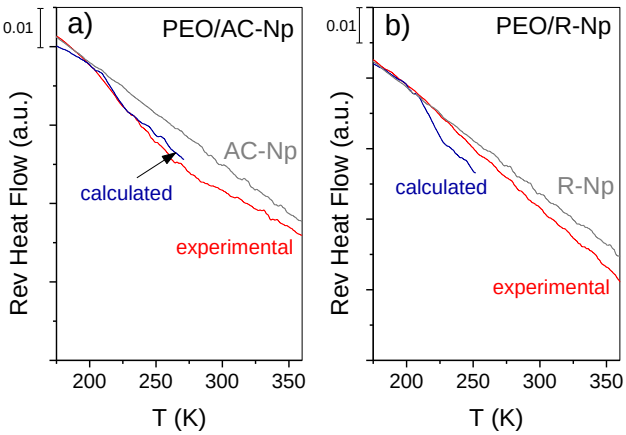

Fig. S13 Blue: calculated DSC curves for PEO/AC-NP and PEO/R-Np, obtained by adding the corresponding DSC response for each component in the sample weighted by its relative abundance. Red: experimental data of PEO/AC-Np and PEO/R-Np. Grey: experimental data of bare substrates.

Inelastic Neutron Spectroscopy

INS data at higher energy transfers of PEO confined in AC−Np is shown in Fig. S14.

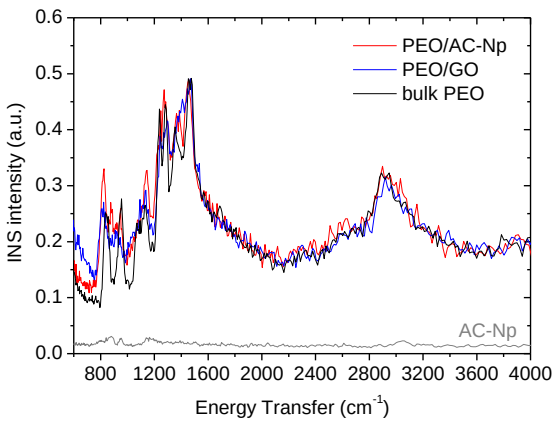

Fig. S14 High-energy region of the mass-normalised INS spectra measured on the TOSCA spectrometer.

References

1 R. W. Pekala, *J. Mater. Sci.*, 1989, **24**, 3221-3227.
2 F. Rouquerol, J. Rouquerol and K. Sing, *Adsorption by powders and porous solids*, Academic Press, San Diego, 1999.
3 S. Brunauer, P. H. Emmett and E. Teller, *J. Amer. Chem. Soc.*, 1938, **60**, 309-319.
4 W. D. Harkins and G. Jura, *J. Chem. Phys.*, 1943, **11**, 431-432.
5 E. P. Barrett, L. G. Joyner and P. P. Halenda, *J. Am. Chem. Soc.*, 1951, **73**, 373-380.
6 J. C. P. Broekhoff and J. H. de Boer, *J. Catal.*, 1968, **10**, 368-376.
7 D. Colognesi, M. Celli, F. Cilloco, R. J. Newport, S. F. Parker, V. Rossi-Albertini, F. Sacchetti, J. Tomkinson and M. Zoppi, *Appl. Phys. A: Mater. Sci. Process.*, 2002, **74**, s64-s66.